

Color randomization of fast gluon-gluon pairs in the quark-gluon plasma

B.G. Zakharov¹

¹*L.D. Landau Institute for Theoretical Physics, GSP-1, 117940, Kosygina Str. 2, 117334 Moscow, Russia*

(Dated: March 14, 2022)

We study the color randomization of two-gluon states produced after splitting of a primary fast gluon in the quark-gluon plasma. We find that for the LHC conditions the color randomization of the gg pairs is rather slow. At jet energies $E = 100$ and 500 GeV, for typical jet path length in the plasma in central Pb+Pb collisions, the $SU(3)$ -multiplet averaged color Casimir of the gg pair differs considerably from its value $2N_c$ for a fully randomized gg state. Our calculations of the energy dependence for generation of the nearly collinear decuplet gg states, that can lead to the baryon jet fragmentation, show that the contribution of the anomalous decuplet color states to the baryon production should become small at $p_T \gtrsim 10$ GeV.

PACS numbers:

I. INTRODUCTION

The results of experiments on heavy ion collisions at RHIC and LHC provide strong evidence for formation of a hot quark-gluon plasma (QGP) at the proper time $\tau_0 \sim 0.5 - 1$ fm. One of the major signals of the QGP formation in AA collisions is a strong suppression of high- p_T particles (jet quenching (JQ)) as compared to pp collisions. The JQ phenomenon is believed to be a consequence of medium modification of the jet fragmentation functions (FFs) due to radiative [1–6] and collisional [7] parton energy loss in the QGP. The energy loss is dominated by the radiative mechanism, and the effect of the collisional energy loss turns out to be relatively small [8, 9].

The first-principle calculation of the medium modification of the jet FFs in AA collisions remains an unsolved problem. The available approaches to the radiative energy loss [2–5] deal with one gluon emission. In phenomenological applications to the JQ multiple gluon emission is usually treated in the approximation of independent gluon radiation [10], similarly to the radiation of soft photons in QED. This approximation may be reasonable for calculation of the nuclear modification factor R_{AA} that is sensitive mostly to the Sudakov suppression of the FFs at the fractional momenta x close to unity. But this may be unsatisfactory for the soft region $x \ll 1$. In principle, the diagram technique of the light-cone path integral (LCPI) [3, 11] approach, originally developed for one-gluon emission, allows one to go beyond the one gluon level. However, even at the level of two gluons, and in a crude oscillator approximation [12] (when multiple scattering is described in terms of the transport coefficient \hat{q} [2]), calculations become extremely complicated [13–15]. And until now no accurate method has been developed for multiple gluon emission that could be used for a robust calculation of the in-medium jet evolution. In the last years many efforts have been and are being made on developing the Monte-Carlo models of the in-medium parton cascading (see e.g. Refs. [16–19]). These models may be successful in the data analyses but solid theoretical support for the probabilistic picture, assumed in the Monte-Carlo schemes, is absent.

The problem of the in-medium jet dynamics is complicated by the lack of an ordering of scales (say, like the angular ordering for the vacuum parton cascade) for the induced gluon emission. It is important that, in principle, for parton cascade in a finite-size medium it is impossible to separate the cases of the ordinary virtuality-ordered parton splittings and that induced by parton rescatterings on the medium constituents. For this reason a consistent treatment should deal with the full medium modified parton cascade. At one gluon emission level the induced contribution to the gluon spectrum may be defined as a difference between the spectrum in the medium and the vacuum one. But this procedure is rather formal, because this difference includes interference between the vacuum parton splitting without interaction with the medium and the parton splitting accompanied by parton rescatterings in the medium. The interference effects are important at $L \lesssim L_f^{in}$, where L_f^{in} is the typical formation length for the induced gluon emission in a uniform medium. Only at large distance from the jet production point, when the interference terms become small, one may speak of the purely induced gluon emission. It is important that for RHIC and LHC conditions, even for soft gluons with energy $\omega \lesssim 3 - 5$ GeV that dominate the induced energy loss, L_f^{in} may be rather large $\sim 2 - 5$ fm¹. Since this scale is not small as compared to the size and life-time of the QGP for RHIC and LHC conditions, we have

¹ For an infinite uniform QGP $L_f^{in} \sim 2\omega S_{LPM}/m_g^2$, where S_{LPM} is the Landau-Pomeranchuk-Migdal suppression factor and m_g is the gluon quasiparticle mass. For RHIC and LHC conditions typically $S_{LPM} \sim 0.3 - 0.5$ for $m_g \sim 400$ MeV [20]. Then we find that $L_f^{in} \sim 2 - 5$ fm at $\omega \sim 3 - 5$ GeV.

a situation when inside the QGP the interference between the vacuum amplitudes and the ones with rescatterings is important. However, if the QGP production time $\tau_0 \sim 0.5 - 1$ fm [21], one can expect that for jets with $E \lesssim 100$ GeV the first most energetic radiated gluon should not be affected strongly, because the typical formation length for such gluons turns out to be of the order of (or smaller) than τ_0 [22]. But subsequent evolution of the two parton system produced in the primary parton splitting should be affected by the medium effects.

It is important that the t -channel gluon exchanges between the fast partons and the QGP constituents, even for very small momentum kicks, can affect the angular-ordered jet evolution. One of the mechanisms for this is violation of the color coherence for the in-medium parton splitting that destroys the angular ordering inherent to the vacuum cascade. In Ref. [23] it was shown that the disruption of the angular ordering leads to a substantial softening of the intrajet rapidity spectrum. For jets with $E \lesssim 100$ GeV for which, as was said before, the formation length for the first parton branching is small, the medium color decoherence/randomization comes into play for gluon emission from the two-parton states created after decay of the initial hard parton. One more mechanism for the medium modification of the jet FFs is connected with change of the total jet color charge by the t -channel gluon exchanges. The t -channel gluons do not change the total color charge for a single fast parton. But already after the first in-medium splitting of the primary parton, the created two-parton system may belong to a color multiplet that is impossible for the vacuum cascade (when for quark and gluon jets the triplet and octet color states persist for the whole parton cascade). This is illustrated in Fig. 1 for $g \rightarrow gg$ splitting. The change in the jet color charge may lead to modification of the jet FFs due to change in the hadronization pattern for fast partons after escaping from the QGP [24–26]. In Refs. [25, 26] this mechanism has been discussed for $N = 1$ and $N = 2$ rescatterings from the point of view of the large- N_c limit using the cluster and LUND hadronization models. It was shown that the medium-modified color flow can contribute to the quenching of hadron spectra, and increase the jet FFs in the soft region.

Production of the nearly collinear gg systems (for quark jets) in the $\{6\}$ color state and of the gg systems (for gluon jets) in the $\{10\}$ and $\{\bar{10}\}$ color states can lead to an interesting mechanism of the leading baryon production in jet fragmentation [24, 27]. Because after escaping from the QGP these states may result in creation of color tubes with the same anomalous color flux. The breaking of these color flux tubes via the Schwinger tunnel $q\bar{q}$ pair creation produces the color string configurations with the string junction, which traces the baryon number in the topological expansion scheme [28, 29], that should hadronize into a system with a leading baryon. This mechanism of the baryon jet fragmentation for the decuplet gg pairs is illustrated in Fig. 2 (the interested reader is referred to Ref. [24] for extensive discussion on this mechanism). An accurate calculation of the contribution of this mechanism to the baryon production in AA collisions is impossible. But qualitative analysis performed in Ref. [24] indicates that this mechanism may give a considerable contribution to the anomalous baryon production at intermediate p_T observed in AA collisions at RHIC and LHC [30–32]. The calculations of Ref. [24] have been performed under assumption of a fast randomization of the two-parton states in the QGP. However, the approximation of the fully color randomized state becomes invalid for sufficiently high energies, when the transverse size of the gg pair remains small (say, as compared to the Debye radius of the QGP) on the longitudinal scale about the typical jet path length in the QGP. To understand better the role of the anomalous color states in the baryon jet fragmentation it would be interesting to perform a quantitative analysis of the color randomization of two-parton states.

A quantitative analysis of the color randomization of two-parton states is also of interest in connection with the role of the color decoherence in the in-medium soft gluon emission by a two-parton antenna that depends crucially on the rate of the antenna color randomization. Over the last years the gluon emission from the two-parton antennas has been used actively as an interesting theoretical laboratory to explore the in-medium multiple gluon emission (see, e.g. [33–36]). These studies show that, similarly to the vacuum parton cascade [37], the coherence effects are very important in multiple in-medium gluon emission. Usually the color randomization of the two-parton antenna is described by a single parameter: the decoherence time that characterizes the exponential reduction of the probability for antenna to stay in the initial color multiplet. But it would be of interest to see in more detail how the color randomization goes. Say, to understand the L -dependence of the distribution of the two-parton state in the irreducible color multiplets. This distribution, e.g., is crucial for emission of gluons with the inverse gluon transverse momentum larger than the transverse size of the two-parton system, which is only sensitive to the total jet color charge (both for the vacuum gluon emission [37] from fast partons after escaping from the QGP and for the in-medium one [38]). The information on the magnitude of the color decoherence in the QGP may also be useful in building of a qualitative picture of what goes on with jets in AA collisions in the whole phase space [38–40] and for development of the Monte-Carlo models that account (at least qualitatively) for the decoherence effects, e.g. like that of Ref. [23].

In the present paper we perform analysis of the color randomization for a gg pair produced from the decay of a primary high energy gluon. We perform calculation for the QGP corresponding to conditions of central Pb+Pb collisions at the LHC energy $\sqrt{s} = 2.76$ TeV. We describe the color randomization with the help of evolution equation for the color density matrix for the gg system. The diffraction operator for the four-gluon system, which is a crucial ingredient for our calculations, has been previously calculated in Ref. [41], devoted to the forward gluon-gluon di-jet production in pA collisions.

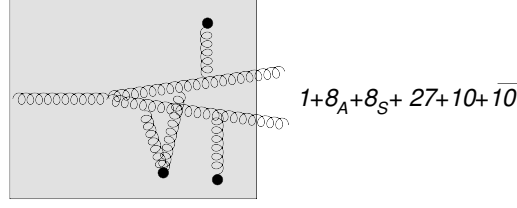


FIG. 1: The $g \rightarrow gg$ in-medium splitting and possible color states of the final two-gluon system.



FIG. 2: (left) The color string configuration created by the right-moving fast gg pair in the decuplet color state after escaping from the QGP and color neutralization of the color flux via the Schwinger production of three $q\bar{q}$ pairs, J denotes the string junction [28, 29]. (right) The same but after splitting of fast gluons into $q\bar{q}$ pairs.

The plan of the paper is as follows. In Sec. 2 we describe the formalism for evaluation of the L -dependence of the color density matrix of the gg system in the QGP. In Sec. 3 we discuss the model of the QGP fireball and the parametrization of the dipole cross section used in our calculations. In Sec. 4 we present the numerical results. We give conclusions in Sec. 5. Some formulas relevant to our calculations are given in Appendix.

II. EVOLUTION OF THE COLOR DENSITY MATRIX OF gg PAIR

In this section we formulate our model for in-medium evolution of the color state of a two-gluon pair produced via splitting $g \rightarrow gg$ of an initial hard gluon with energy E . We assume that the parent fast gluon is produced at $z = 0$ (we choose z -axis along its momentum, so z equals the jet path length L in the QGP). We will describe the QGP in the approximation of static color Debye-screened scattering centers [1].

In general, in the LCPI formalism [11] the probability of $a \rightarrow bc$ splitting in the small angle approximation may be represented as a path integral over the transverse parton coordinates on the light-cone $t - z = \text{const}$ shown diagrammatically in Fig. 3, where the right and left arrows denote the trajectories for the amplitude and the complex conjugate amplitude, respectively. The color generators for a parton p and for its antipartner \bar{p} satisfy the relation $T_p^\alpha = -(T_{\bar{p}}^\alpha)^*$ (for $p = g$ we have $\bar{g} = g$). With the help of this relation one can show that, in the approximation of two-gluon exchanges between fast partons and medium constituents, the parton lines corresponding to the complex conjugate amplitude interact with the medium similarly to the antiparton lines. It means that in the path integral the interaction part of the Lagrangian is analogous to that for a fictitious system of partons (upper lines in Fig. 3) and antipartons (lower lines in Fig. 3). This system is fictitious because in the Lagrangian the kinetic term for antipartons is negative due to complex conjugation. It is important that the fictitious parton-antiparton system at any z is in a color singlet state. Indeed, since we perform averaging over the color states of the initial hard parton a , at the initial instant $z = 0$ we have the $a\bar{a}$ pair in the color singlet state (this means that the two gluon lines at the initial instant

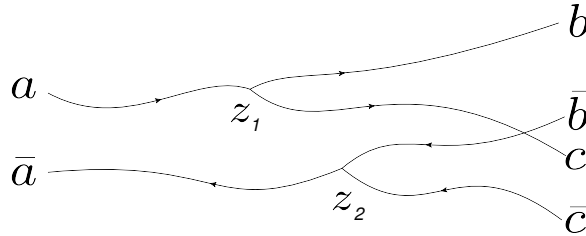


FIG. 3: Schematic diagram picture of the light-path integral representation for the squared amplitude $|\langle bc|T|a\rangle|^2$ describing the probability of $a \rightarrow bc$ transition in the LCPI [11] approach. The lines with right and left arrows correspond to the amplitude and complex conjugate amplitude, respectively. For the in-medium transition the lines can interact with the medium constituents via the t -channel gluon exchanges.

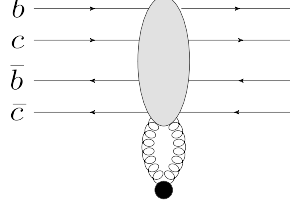


FIG. 4: The diffractive operator for scattering of the four-body $bcb\bar{c}$ system on a medium constituent in the two-gluon approximation. The blob includes all possible attachments of the t -channel gluons to the parton and antiparton lines.

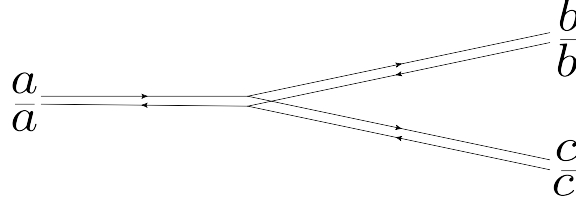


FIG. 5: The parton trajectories for the squared amplitude $|\langle bc|T|a\rangle|^2$ for $a \rightarrow bc$ splitting in the approximation of rigid geometry used in the present analysis.

in Fig. 3 become closed in the sense of the color flow.) And the subsequent t -channel two-gluon exchanges do not change the total color charge of our fictitious system. It occurs because only color singlet two-gluon states survive after summing over the final states of the medium with the help of the closure relation. After this operation is done at the level of the integrand, the effect of the t -channel gluon exchanges² translates to appearance in the Lagrangian for the fictitious parton-antiparton system interaction between the trajectories described by an imaginary potential

$$V(z, \{\boldsymbol{\rho}\}, \{\bar{\boldsymbol{\rho}}\}) = -i \frac{n(z) \hat{\sigma}(z, \{\boldsymbol{\rho}\}, \{\bar{\boldsymbol{\rho}}\})}{2}, \quad (1)$$

where $\{\boldsymbol{\rho}\}$ and $\{\bar{\boldsymbol{\rho}}\}$ are the sets of the transverse coordinates of the partons and antipartons, $n(z)$ is the number density of the medium constituents, and $\hat{\sigma}(z, \{\boldsymbol{\rho}\}, \{\bar{\boldsymbol{\rho}}\})$ is the diffraction operator for scattering of the fictitious system on the medium constituent via the two-gluon exchanges (as shown in Fig. 4 for the four-parton system $bcb\bar{c}$). In (1) (and below) for notational simplicity we omit the sum over species of the medium constituents (quarks and gluons). In the diagram of Fig. 3 for the two-body ($z < z_1$) and three-body ($z_1 < z < z_2$) parton-antiparton systems only one color singlet state is possible³. In both the cases, the color singlet states are the eigenstates of the diffraction operator, for this reason for the two- and three-body parts the diffraction operator may simply be replaced by the total cross sections for the two- and three-body color singlet systems. For the four-body part at $z > z_2$ the situation is more complicated, because there are several color singlet four-parton states, and the diffraction operator has off-diagonal elements between them. For this reason for the four-body part in the diagram of Fig. 3 the path integration over the transverse coordinates cannot be separated from the color algebra.

In the present work we perform calculations using the rigid geometry with the straight trajectories, same for the amplitude and the complex conjugate one as shown in Fig. 5 for $a \rightarrow bc$ transition. This approximation seems to be reasonable for relatively hard parton splittings, when fluctuations of the trajectories of energetic partons are small and the separation between the jet production point for the amplitude and the complex conjugate amplitude ($\sim 1/Q$) is much smaller than the typical scale for color fields in the QGP, say than the Debye radius. The approximation of straight trajectories for fast partons has been widely used for analysis of soft gluon emission in hard QCD process.

² In the literature, the interaction of parton trajectories with QCD matter is often described in terms of the Wilson line factors. This may create an impression that the picture with the fictitious color singlet parton-antiparton system interacting with the medium is valid even for nonperturbative fluctuation of the color fields of the medium. But this is not the case, because for nonperturbative situation the vector potentials in the Wilson lines for the amplitude and in the ones for the complex conjugate amplitude may be different. Even in the perturbation theory the validity of this picture is limited only to the two-gluon t -channel exchanges.

³ For three gluons there are two color singlet states: asymmetric $\propto f_{\alpha\beta\gamma}$ and symmetric $\propto d_{\alpha\beta\gamma}$. However, in the case of the $g \rightarrow gg$ splitting the three-body system in the diagram of Fig. 3 may be only in asymmetric color state, because after $g \rightarrow gg$ transition two gluons are in asymmetric color octet state, and the t -channel gluon exchanges cannot change the symmetry of the three-gluon color wave function.

E.g. this picture has been used in calculations of the anomalous dimension matrix for large angle soft gluon emission in hard $gg \rightarrow gg$ scattering [42–45]. One can say that the approximation of straight lines, in terminology of the recent analysis [40], should be reasonable for the vacuum-like emission. However, we will also apply it to a relatively soft $g \rightarrow gg$ splitting (where its applicability is questionable) for a qualitative analysis of the color decoherence in the induced gluon emission.

In our case of $g \rightarrow gg$ transition the fictitious color singlet four-body $b\bar{c}b\bar{c}$ system is simply a color singlet four-gluon system because gluon is a self-conjugate particle and $gg\bar{g}\bar{g} = gggg$. We will label the final two gluons in the amplitude g_1 and g_2 , and the final two gluons in the complex conjugate amplitude g_3 and g_4 . We describe the color state of the two gluon system by the density matrix $\langle ab|\hat{\rho}|cd\rangle$, where a, b, c and d refer to the color indexes of the gluons g_1, g_2, g_3 and g_4 , respectively.⁴ The imaginary potential (1) in the path integral formulation corresponds to the evolution equation for the two-gluon color density matrix given by

$$\frac{d\hat{\rho}(z)}{dz} = -\frac{n(z)}{2}\hat{\sigma}\hat{\rho}, \quad (2)$$

where $\hat{\sigma}$ is the diffraction operator for scattering of the four-gluon system due to the double gluon exchange as shown in Fig. 4. The color density matrix of the two-gluon system in (2) may be viewed as the color wave function of the fictitious color singlet four-gluon system

$$\langle abcd|\Psi\rangle = \langle ab|\hat{\rho}|cd\rangle. \quad (3)$$

The color wave functions of the gluon pairs g_1g_2 and g_3g_4 may belong to one of the irreducible multiplets in the Clebsch-Gordan decomposition of the direct product of two octets

$$8 \otimes 8 = 1 + 8_A + 8_S + 27 + 10 + \overline{10}, \quad (4)$$

where 8_A and 8_S denote the antisymmetric and symmetric octet states that may be built from the $SU(3)$ tensors $f_{\alpha\beta\gamma}$ and $d_{\alpha\beta\gamma}$, respectively. From the irreducible multiplets in the Clebsch-Gordan decomposition (4) one can build eight color singlet states for the four-gluon system. There are six states of the types $|RR\rangle/|R\bar{R}\rangle$

$$|11\rangle, |8_A8_A\rangle, |8_S8_S\rangle, |2727\rangle, |10\overline{10}\rangle, |\overline{10}10\rangle, \quad (5)$$

and two mixed states built from different octet multiplets

$$|8_A8_S\rangle, |8_S8_A\rangle. \quad (6)$$

The in-medium color randomization of the two-gluon system produced in the process $g \rightarrow gg$ can be described in terms of the six states given in (5) (in our formulas we will denote these states as $|R\bar{R}\rangle$ even for self-conjugate multiplets when $|R\bar{R}\rangle = |RR\rangle$). The point is that the initial two-gluon state for the transition $g \rightarrow gg$ is the antisymmetric octet 8_A . In terms of the description of the density matrix via the four-gluon wave function it corresponds to the color singlet $|8_A8_A\rangle$. The subsequent in-medium evolution of this state (and of any other state of the types $|R\bar{R}\rangle/|RR\rangle$) cannot generate the mixed states (6) because the matrix elements of the diffraction operator $\hat{\sigma}$ between the states from (5) and (6) vanish. This means that the mixed states (6) turn out to be fully decoupled from the color randomization of the two gluon system. Thus, the in-medium four-gluon wave function can be decomposed as a sum over the singlet color states given in (5)

$$\langle abcd|\Psi\rangle = \sum_R c_R \langle abcd|R\bar{R}\rangle. \quad (7)$$

The corresponding decomposition of the density matrix can be written as

$$\langle ab|\hat{\rho}|cd\rangle = \sum_R P_R \langle ab|\hat{\rho}_R|cd\rangle, \quad (8)$$

⁴ Note that we consider the situation when the color indexes for final gluons in the amplitude and the complex conjugate amplitude may differ. This differs from calculation of the gluon spectrum, when one performs summing over $a = c$ and $b = d$ [11, 46, 47], and the final gluon lines with right and left arrows in Figs. 3, 5 become closed (in the sense of the color flows).

where P_R is the probability that the two-gluon system belongs to the multiplet R , and $\hat{\rho}_R$ is the density matrix for the multiplet R . The full density matrix $\hat{\rho}$ and its components $\hat{\rho}_R$ satisfy the normalization conditions

$$\sum_{a,b} \langle ab | \hat{\rho} | ab \rangle = 1, \quad \sum_{a,b} \langle ab | \hat{\rho}_R | ab \rangle = 1. \quad (9)$$

The z -dependence of the vector

$$\vec{P} = (P_1, P_{8_A}, P_{8_S}, P_{27}, P_{10}, P_{\overline{10}}) \quad (10)$$

characterizes the process of the in-medium color randomization of the gg pair. The in-medium evolution should satisfy the conservation of the total probability to find the gg pair in any color state

$$\sum_R P_R = 1. \quad (11)$$

In the limit of very large medium thickness the gg pair should tend to the fully color randomized state, when P_R is defined by the multiplet dimensions

$$P_R|_{\text{randomized}} = \frac{\dim[R]}{\sum_{R'} \dim[R']} = \frac{\dim[R]}{(N_c^2 - 1)^2}. \quad (12)$$

The normalized to unity density matrix $\hat{\rho}_R$ for a given multiplet R can be written as

$$\langle ab | \hat{\rho}_R | ab \rangle = \frac{1}{\dim[R]} P[R]_{cd}^{ab}, \quad (13)$$

where

$$P[R]_{cd}^{ab} = \sum_{\nu} \langle ab | R\nu \rangle \langle R\nu | cd \rangle \quad (14)$$

is the projector onto the states of the irreducible multiplet R (here ν labels the states in the multiplet R). The fact that $\hat{\rho}_R$ given in (13) is normalized to unity is a consequence of the relation

$$\sum_{a,b} P[R]_{ab}^{ab} = \dim[R]. \quad (15)$$

The derivation of the formulas for the projectors can be found in Refs. [41, 44]. For the reader's convenience we present them in Appendix.

The four-gluon color wave function $\langle abcd | R\bar{R} \rangle$ in terms of the projector $P[R]_{cd}^{ab}$ reads

$$\langle abcd | R\bar{R} \rangle = \frac{1}{\sqrt{\dim[R]}} P[R]_{cd}^{ab}. \quad (16)$$

From the fact that $P[R]P[R] = P[R]$ and the relation (15) one can see that the wave function (16) is normalized to unity, i.e.

$$\sum_{abcd} \langle R\bar{R} | abcd \rangle \langle abcd | R\bar{R} \rangle = 1. \quad (17)$$

We explicitly show here the sum over the gluon color states to demonstrate that the normalizations conditions for the components of the density matrix for a given multiplet $\langle ab | \hat{\rho}_R | cd \rangle$ and the color singlet four-gluon wave function $\langle abcd | R\bar{R} \rangle$ built from R and \bar{R} are defined in different ways.

From (2) and (3) one can easily obtain the evolution equation in terms of the coefficients c_R in the four-gluon wave function decomposition into the $R\bar{R}$ states (7)

$$\frac{dc_R}{dz} = -\frac{n(z)}{2} \langle R\bar{R} | \hat{\sigma} | R' \bar{R}' \rangle c_{R'}. \quad (18)$$

The formulas for the diffraction operator in the basis of the color singlet states $|R\bar{R}\rangle$ for arbitrary gluon positions have been derived in [41]. For the reader's convenience in Appendix we present the formula for the diffraction matrix

$\langle R\bar{R}|\hat{\sigma}|R'\bar{R}'\rangle$ for the gluon configurations for the rigid geometry (as shown in Fig. 5) with the transverse coordinates $\mathbf{b}_1 = \mathbf{b}_3$ and $\mathbf{b}_2 = \mathbf{b}_4$, that is used in the present analysis. Note that the off-diagonal elements of the diffraction operator are nonzero only between the multiplets with different permutation symmetry. From (13), (16) one can see that the relation between the coefficients c_R in the decomposition of the wave function (7) and the coefficients P_R in the decomposition of the density matrix (8) reads

$$c_R = P_R / \sqrt{\dim[R]}. \quad (19)$$

Then, the evolution equation (18) in terms of the coefficients P_R can be written as

$$\frac{dP_R}{dz} = -\frac{n(z)}{2} \langle R\bar{R}|\hat{\sigma}|R'\bar{R}'\rangle P_{R'} \sqrt{\frac{\dim[R]}{\dim[R']}}. \quad (20)$$

It worth noting that, in the description of the in-medium evolution in terms of the four-gluon wave function, $\langle \Psi|\Psi\rangle = \sum_R |c_R|^2$ does not corresponds to the total probability to find the two-gluon system in any color state. And the evolution equation (18) does not conserve $\sum_R |c_R|^2$. The total probability to find the two-gluon system in any color state is given by the sum $\sum_R P_R$. The fact the evolution equation (20) preserves the probability conservation for P_R (11) is a non-trivial consequence of the color transparency for the point-like color singlet parton states. Indeed, from (20) one can see that the conservation of the sum $\sum_R P_R$ requires fulfilling the relation

$$\sum_R \langle R\bar{R}|\hat{\sigma}|R'\bar{R}'\rangle \sqrt{\dim[R]} = 0 \quad (21)$$

for any R' . One can write the left-hand side of (21) as

$$\sum_R \langle R\bar{R}|abcd\rangle \langle abcd|\hat{\sigma}|R'\bar{R}'\rangle \sqrt{\dim[R]} = \sum_R P[R]_{cd}^{ab} \langle abcd|\hat{\sigma}|R'\bar{R}'\rangle. \quad (22)$$

But from the closure relation for the projectors

$$\sum_R P[R]_{cd}^{ab} = \mathbb{1}_{cd}^{ab} = \delta_{ac}\delta_{bd}, \quad (23)$$

one obtains for the left-hand side of (22)

$$\sum_{ab} \langle abab|\hat{\sigma}|R'\bar{R}'\rangle \propto \langle (g_1g_3)_{\{1\}}(g_2g_4)_{\{1\}}|\hat{\sigma}|R'\bar{R}'\rangle, \quad (24)$$

where $(g_1g_3)_{\{1\}}$ and $(g_2g_4)_{\{1\}}$ denote the color singlet states of the gluon pairs g_1g_3 and g_2g_4 . In our case these pairs have a zero size. For such configurations the total contribution of the t -channel two-gluon exchanges should vanish. This proves the conservation of the sum $\sum_R P_R$. Note that the above consideration also works to prove that for the vector (10) with P_R for the regime of complete color randomization defined by (12) the right-hand side of (20) vanishes (it means that (12), in terms of the coefficients c_R , corresponds to the eigenvector of the diffraction operator with zero eigenvalue). Indeed, for $P_{R'}$ defined by (12) the right-hand side of (20) is proportional to

$$\sum_{R'} \langle R\bar{R}|\hat{\sigma}|R'\bar{R}'\rangle \sqrt{\dim[R']} \quad (25)$$

that, similarly to (21), vanishes for any multiplet R .

The above formulas correspond to the color singlet four-gluon states written in terms of the color states of the gluon pairs g_1g_2 and g_3g_4 . But one can describe the four-gluon system in terms of the color singlet states constructed from the pairs g_1g_3 and g_2g_4 . As in Ref. [41] we call these two bases the s - and t -channel bases. The t -channel basis states can be obtained from the s -channel ones by a unitary transformation U_{ts} (and the inverse matrix U_{st} transforms the t -channel states into the s -channel states). Since the complete set of the color singlet four-gluon states includes the mixed states (6), the dimension of the crossing matrix U_{ts} is 8×8 . The matrix U_{ts} was calculated in [41]. For the reader's convenience we present U_{ts} in Appendix (we correct some misprints in the formula C17 of Ref. [41]). It is convenient to write the crossing matrix using for the mixed states (6) the linear combinations

$$|(8_A8_S)_{\pm}\rangle = \frac{i}{\sqrt{2}} (|8_A8_S\rangle \pm |8_S8_A\rangle). \quad (26)$$

In this basis the t -channel state $|(8_A 8_S)^-\rangle$ has a non-zero projection only on the same s -channel state $|(8_A 8_S)^-\rangle$, and the state $|(8_A 8_S)^+\rangle$ in the t -channel basis has non-zero projections only on the states $|10\bar{1}0\rangle$ and $|\bar{1}010\rangle$ in the s -channel basis. By appropriate choice of the phase factors for the $|8_A 8_S\rangle$ and $|8_S 8_A\rangle$ states, the unitary crossing matrix can be made real and symmetric, i.e., we have $U_{ts} = U_{st}$ and $U_{ts}^2 = \mathbb{1}$ (see Appendix for details). Note that this is possible only for the complete set of the color singlet states, i.e., for the 8×8 crossing matrix.

The solution of the evolution equation (18) can be expressed via the eigenfunctions of the diffraction matrix. The eigenvectors can be easily written in terms of the t -channel states analogous to (5) and the linear combinations (26) of the $8_A 8_S$ and $8_S 8_A$ states. The point is that $g_1 g_3$ and $g_2 g_4$ pairs are the point-like objects. For this reason the t -channel gluons cannot resolve their internal color structure, and do not change the color multiplets for $g_1 g_3$ and $g_2 g_4$ pairs. As a result, the diffraction operator in the t -channel basis $|\Psi_i^t\rangle$ has a simple diagonal form with

$$\langle \Psi_i^t | \hat{\sigma} | \Psi_j^t \rangle = \delta_{ij} \sigma_{R_i}(\rho_{12}), \quad (27)$$

where R_i denotes the color multiplet the state Ψ_i^t is built from, and σ_{R_i} is the dipole cross section for the color singlet state $R_i \bar{R}_i$ (from the point of view of the dipole cross section there is no difference between 8_A and 8_S octets), $\rho_{12} = |\mathbf{b}_1 - \mathbf{b}_2|$ is the transverse size of the $g_1 g_2$ pair (which equals to that for the $g_3 g_4$ pair). In the approximation of the static Debye-screened scattering centers [1] the dipole cross section for the color singlet $R \bar{R}$ state reads

$$\sigma_R(\rho) = C_T C_R \int d\mathbf{q}_\perp \alpha_s^2(\mathbf{q}_\perp^2) \frac{[1 - \exp(i\mathbf{q}_\perp \rho)]}{(\mathbf{q}_\perp^2 + m_D^2)^2}, \quad (28)$$

where m_D is the Debye mass, C_T and C_R are the color Casimir operators for the QGP constituent and the multiplet R . The $SU(3)$ Casimir operators that we need read: $C_1 = 0$, $C_8 = N_c$, $C_{10} = 2N_c$, $C_{27} = 2(N_c + 1)$. The six eigenstates of the diffraction operator in the s -channel basis can be obtained by acting with the crossing matrix U_{st} on the t -channel states

$$|11\rangle_t, |8_A 8_A\rangle_t, |8_S 8_S\rangle_t, |(8_A 8_S)_+\rangle_t, |27\,27\rangle_t, (|10\bar{1}0\rangle_t + |\bar{1}010\rangle_t)/\sqrt{2}. \quad (29)$$

For each eigenstate the medium effect is reduced to trivial multiplication by the Glauber attenuation factor

$$S_R(z, z_s) = \exp \left[-\frac{1}{2} \int_{z_s}^z dz n(z) \sigma_R(\rho_{12}(z)) \right], \quad (30)$$

where z_s is the longitudinal coordinate of the $g \rightarrow gg$ splitting, R is the multiplet entering the t -channel state. The eigenstate corresponding to the state $|(8_A 8_S)_+\rangle_t$ in terms of the s -channel basis is $(|10\bar{1}0\rangle - |\bar{1}010\rangle)/\sqrt{2}$, i.e., it describes the difference between the probabilities for the decuplet P_{10} and the antidecuplet states $P_{\bar{1}0}$. Since for the $g \rightarrow gg$ splitting at initial instant $P_{10} = P_{\bar{1}0}$, one can simply ignore this state. Then, the z -dependence of the coefficients c_R in the s -channel basis can be written as

$$c_R(z) = \sum_{R', R_0} \langle R \bar{R} | U_{st} | R' \bar{R}' \rangle S_{R'}(z, z_s) \langle R' \bar{R}' | U_{ts} | R_0 \bar{R}_0 \rangle c_{R_0}(z_s), \quad (31)$$

where sum over the intermediate t -channel states includes only the first six states of the type $|R \bar{R}\rangle$. Thus, for $g \rightarrow gg$ splitting we need only 6×6 block of the full 8×8 crossing matrix. From (31) we obtain for the vector \vec{P}

$$P_R(z) = \sum_{R', R_0} \langle R \bar{R} | U_{st} | R' \bar{R}' \rangle S_{R'}(z, z_s) \langle R' \bar{R}' | U_{ts} | R_0 \bar{R}_0 \rangle P_{R_0}(z_s) \sqrt{\frac{\dim[R]}{\dim[R_0]}}. \quad (32)$$

In the limit of very large thickness in (31), (32) in the sum over the intermediate t -channel states only the $|11\rangle$ state with $\sigma_1 = 0$ and $S_1 = 1$ survives, and one can write (32) at $z \rightarrow \infty$ as

$$P_R(z)|_{z \rightarrow \infty} \approx \sum_{R_0} \langle R \bar{R} | U_{st} | 11 \rangle \langle 11 | U_{ts} | R_0 \bar{R}_0 \rangle P_{R_0}(z_s) \sqrt{\frac{\dim[R]}{\dim[R_0]}}. \quad (33)$$

The t -channel color singlet wave function is given by $\langle abcd | 11 \rangle = \delta_{ac} \delta_{bd} / (N_c - 1)^2$. Using this formula with the help of (15) and (16) one obtains $\langle R \bar{R} | U_{st} | 11 \rangle = \sqrt{\dim[R]} / (N_c^2 - 1)$, and a similar formula for $\langle 11 | U_{ts} | R_0 \bar{R}_0 \rangle$. Then, with these matrix elements the right-hand side of (33) is reduced to the color randomized distribution (12).

For the initial two-gluon state produced via the gluon splitting $g \rightarrow gg$ in the right-hand side of (31) and (32) there is no summing over R_0 because in this case we have only one non-zero component for $R_0 = 8_A$ with $P_{8_A} = 1$.

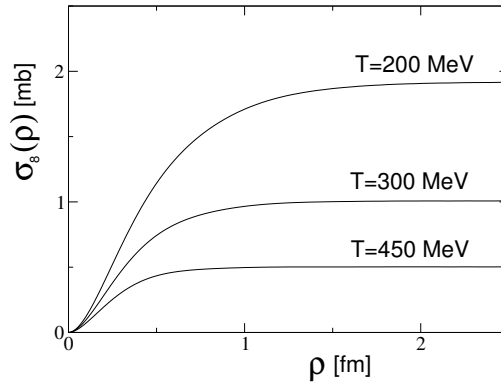


FIG. 6: The octet-octet dipole cross section on a quark in the QGP versus the dipole size ρ for different values of the QGP temperature T .

III. MODEL OF THE QGP FIREBALL AND THE DIPOLE CROSS SECTION

We perform numerical calculations for the model of the QGP fireball with Bjorken's 1+1D expansion [48], that, for the ideal gas model, gives $T_0^3 \tau_0 = T^3 \tau$, where τ_0 is the thermalization time of the matter. As in our previous analyses of the JQ phenomenon [22, 49, 50], we take $\tau_0 = 0.5$ fm, and for simplicity we neglect variation of T_0 with the transverse coordinates. To account for the fact that the QGP formation is clearly not an instantaneous process, we take the medium density $\propto \tau$ at $\tau < \tau_0$. We fix the initial QGP temperature from the initial entropy density determined via the charged particle multiplicity pseudorapidity density, $dN_{ch}^{AA}/d\eta$, at mid-rapidity ($\eta = 0$) with the help of the Bjorken relation [48]

$$s_0 = \frac{C}{\tau_0 S_f} \frac{dN_{ch}^{AA}}{d\eta}. \quad (34)$$

Here $C = dS/dy / dN_{ch}^{AA}/d\eta \approx 7.67$ [51] is the entropy/multiplicity ratio, and S_f is the transverse area of the QGP fireball. For the central Pb+Pb collisions at $\sqrt{s} = 2.76$ TeV this procedure for the ideal gas model gives $T_0 \approx 420$ MeV (we take $N_f = 2.5$ to account for the mass suppression for the strange quarks in the QGP). For the above value of T_0 in 1 + 1D Bjorken's expansion the QGP reaches $T \sim T_c$ (here $T_c \approx 160$ is the crossover temperature) at $\tau_{QGP} \sim 10$ fm. This means that the matter remains in the plasma phase until a strong cooling of the matter at $\tau \gtrsim (1-2)R_A$ (here $R_A \sim 6$ fm is the nucleus radius), when the transverse expansion becomes very strong [48].

In our calculations the properties of the QGP enter only through the product of the number density of the QGP and the dipole cross section in the formula for the Glauber attenuation factors (30). Since the dipole cross section is proportional to the Casimir operator of the scattering center, in this product one can avoid summing over the species of the QGP constituents by using the dipole cross section for scattering on a quark and using, at the same time, for the number density of the color centers the sum $n = n_q + n_g C_A/C_F$ (here n_q is the number density of quarks and antiquarks, and n_g is the number density of gluons, C_A and C_F are the gluon and quark Casimir operators). In calculating the dipole cross section we use the Debye mass m_D in the QGP obtained in the lattice analysis [52], that gives m_D/T slowly decreasing with T ($m_D/T \approx 3$ at $T \sim 1.5T_c$, $m_D/T \approx 2.4$ at $T \sim 4T_c$). As in our analyses [22, 49, 50] of JQ we use the one-loop running α_s frozen at low momenta at some value α_s^{fr} . The analyses of the low- x structure functions [53] and of the heavy quark energy loss in vacuum [54] show that for gluon emission in vacuum for this parametrization $\alpha_s^{fr} \approx 0.7-0.8$. But in the QGP the thermal effects can suppress the in-medium QCD coupling. Our analysis of the LHC data on the nuclear modification factor R_{AA} for Pb+Pb collisions at $\sqrt{s} = 2.76$ TeV within the LCPI approach to the induced gluon emission gives the value $\alpha_s^{fr} \approx 0.4$ [49]. We will use this value in this work. In Fig. 6 we plot the ρ -dependence of the dipole cross section for gg state obtained for several values of the QGP temperature. At small ρ (say, $\lesssim 0.1$ fm) the dipole cross section has nearly quadratic form $\sigma_8(\rho) \approx C\rho^2$, where C depends logarithmically on ρ . In terms of the transport coefficient \hat{q} [2] and the effective number density of the triplet color scattering centers one can write $C = \hat{q}/2n$. Our $\sigma_8(\rho)$ for $\rho \sim 0.1$ fm corresponds to $\hat{q} \sim 0.25$ at $T = 250$ MeV. It agrees reasonably with the qualitative pQCD calculations of Ref. [55] $\hat{q} \sim 2\varepsilon^{3/4}$ with ε the QGP energy density (in terms the QGP temperature it is $\hat{q} \approx 15T^3$).

From Fig. 6 one sees that the dipole cross section flattens at $\rho \sim 2/m_D \sim 1/T$. Fig. 6 shows that between the quadratic and flat regions there is a rather broad region where the dipole cross section is approximately $\propto \rho$. Note that for the regimes with the dipole cross section $\propto \rho^2(\rho)$, for a given transverse momentum of the gg pair and the

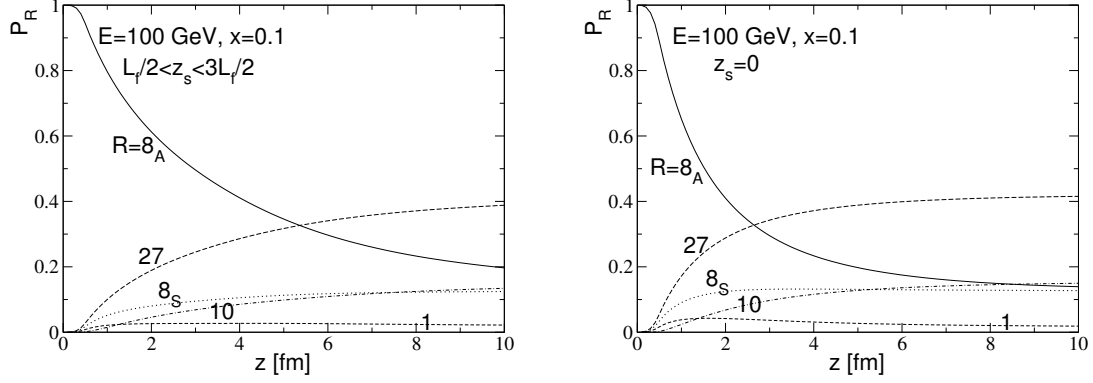


FIG. 7: Coefficients P_R for $g \rightarrow gg$ splitting with $x = 0.1$ averaged over the transverse momentum versus the jet path length for the initial gluon energy $E = 100$ GeV (see main text for details). Left: The position of the splitting point in the interval $L_f/2 < z_s < 3L_f/2$. Right: The splitting at $z_s = 0$. Dashed: $R = 1$; Solid: $R = 8_A$; Dotted: $R = 8_S$; Long-dashed: $R = 27$; Dot-dashed: $R = 10$.

longitudinal coordinate of the splitting point z_s , the probability of the off-diagonal transitions falls approximately $\propto 1/E^{2N}(1/E^N)$, where N is the number of rescatterings. For this reason, as will be seen below, the production of the decuplet gg states, that requires $N \geq 2$, falls steeply with the jet energy.

IV. NUMERICAL RESULTS

We perform analysis of the z -dependence of the probability distribution vector \vec{P} for the gg state averaged over the internal momentum of the gg system. We describe the gluon (x, \mathbf{q}) -distribution for the $g \rightarrow gg$ transition by the leading order pQCD formula

$$\frac{dN}{dx d\mathbf{q}} = \frac{C_A \alpha_s(q^2)}{\pi^2} \left[\frac{1-x}{x} + \frac{x}{1-x} + x(1-x) \right] \frac{q^2}{(q^2 + \epsilon^2)^2}, \quad (35)$$

where C_A is the gluon color Casimir factor, and $\epsilon^2 = m_g^2(1-x+x^2)$. Here the effective gluon mass m_g plays the role of the infrared cutoff. For numerical computations we take $m_g = 0.75$ GeV. This value was obtained from the analysis of the low- x proton structure function F_2 within the dipole BFKL equation [53]. It agrees well with the natural infrared cutoff for perturbative gluons $m_g \sim 1/R_c$, where $R_c \approx 0.27$ fm is the gluon correlation radius in the QCD vacuum [56]. For a given x we restrict the value of q by $q_{max} = Ex(1-x)$, where E is the energy of the parent gluon. In calculation of the distribution (35) we use α_s frozen at the value $\alpha_s^{fr} = 0.7$. This value was previously obtained by fitting the data on proton structure function F_2 at low x within the dipole BFKL equation [53]. This value is also consistent with the relation

$$\int_0^{2 \text{ GeV}} dQ \frac{\alpha_s(Q^2)}{\pi} \approx 0.36 \text{ GeV} \quad (36)$$

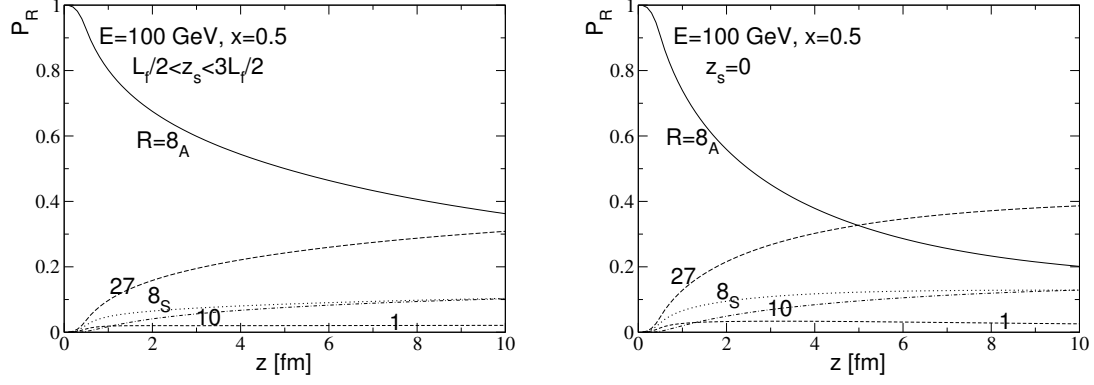
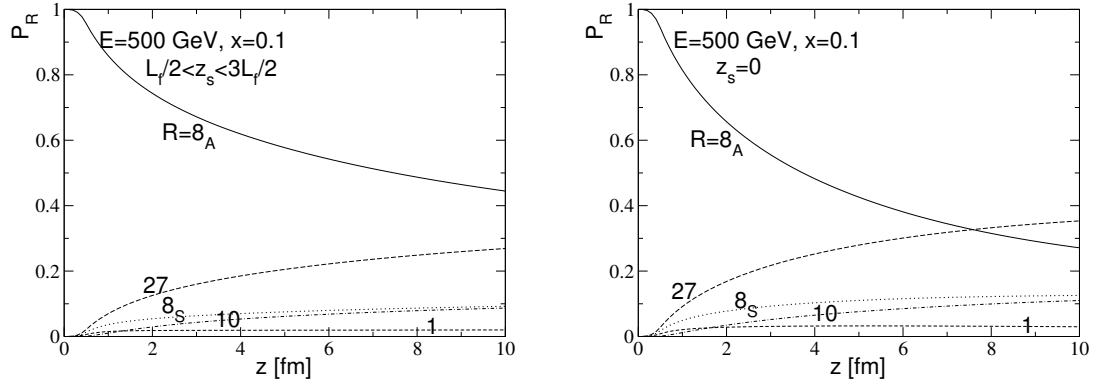
obtained in [54] from the analysis of the heavy quark energy loss in vacuum.

We define the q -averaged P_R as

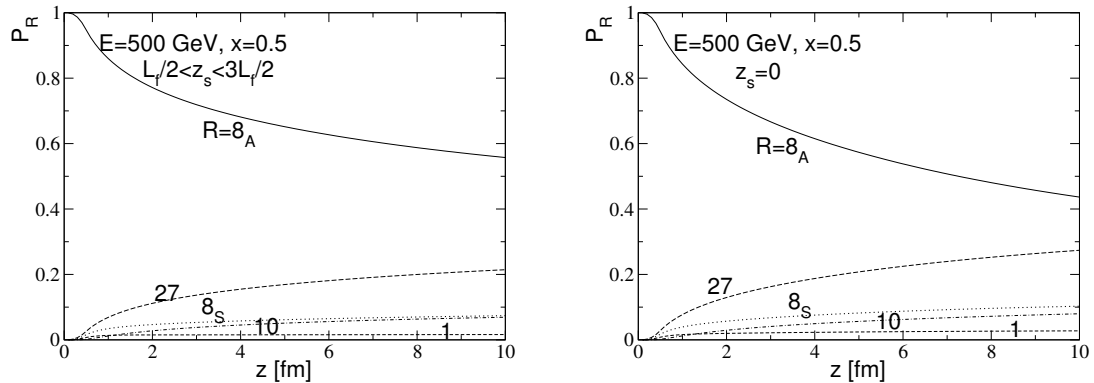
$$P_R(z) = \frac{\int d\mathbf{q} P_R(z, q) \frac{dN}{dx d\mathbf{q}}}{\int d\mathbf{q} \frac{dN}{dx d\mathbf{q}}}, \quad (37)$$

where $P_R(z, q)$ is the solution to the evolution equation (20) for a given geometry of the $g \rightarrow gg$ splitting. The transverse momentum q defines the angle between gluon momenta of the final gg pair. The geometry of the gluon trajectories also depends on the longitudinal coordinate z_s of the splitting point. From the uncertainty relation $\Delta p_z \Delta z \sim 1$ one can obtain for the typical formation length of the gg pair

$$L_f \sim \frac{2x(1-x)E}{q^2 + \epsilon^2}. \quad (38)$$

FIG. 8: Same as in Fig. 7, $E = 100$ GeV, $x = 0.5$.FIG. 9: Same as in Fig. 7, $E = 500$ GeV, $x = 0.1$.

We perform computations for two versions: for instant decay of the primary gluon, i.e., $z_s = 0$, and delayed decay, when the splitting point is uniformly distributed in the interval $L_f/2 < z_s < 3L_f/2$. In Figs. 7–10 we present the results for $P_R(z)$ obtained for $E = 100$ and 500 GeV for $g \rightarrow gg$ splitting with $x = 0.1$ and 0.5 . As one can see, the color randomization becomes stronger with decreasing fractional longitudinal momentum x . It is due to growth of the angle between gluons in the asymmetric gg pairs. For the version with the delayed decay the color randomization is noticeably weaker than that for the instant decay. However, even in the latter case the color randomization of the two gluon system turns out to be rather slow. For example, one can see that for the typical jet path length $L \sim 5$ fm for central Pb+Pb collisions the probability for the gg pair to stay in the 8_A state differs substantially from that in the regime of the full color randomization (especially for symmetric splitting). From Figs. 7–10 one sees that the color randomization is weakest for the decuplet states. This occurs because, contrary to the multiplets 1 , 8_S , 27 , the

FIG. 10: Same as in Fig. 7, $E = 500$ GeV, $x = 0.5$.

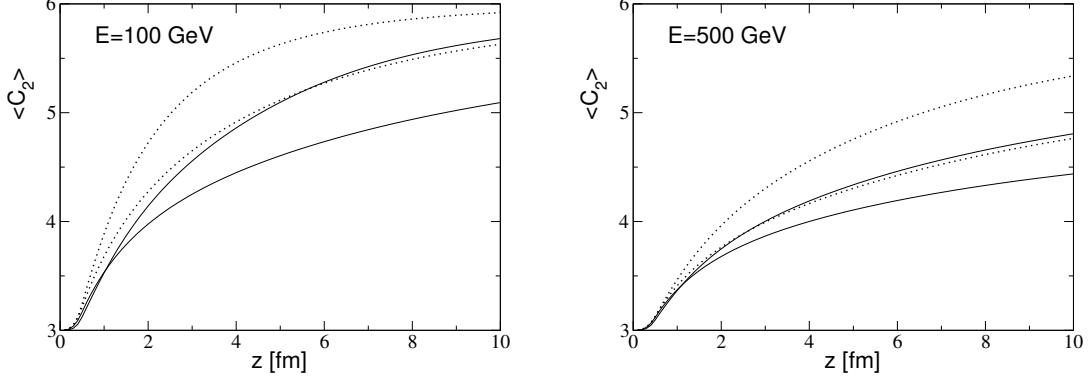


FIG. 11: The multiplet-averaged Casimir operator $\langle C_2 \rangle$ for $g \rightarrow gg$ splitting with $x = 0.1$ and $x = 0.5$ (from top to bottom) at $E = 100$ GeV (left) and $E = 500$ GeV (right) versus the jet path length obtained for the splitting point in the interval $L_f/2 < z_s < 3L_f/2$ (solid) and for the splitting at $z_s = 0$ (dashed).

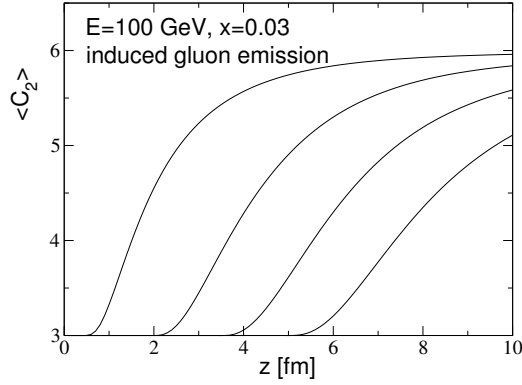


FIG. 12: The multiplet-averaged Casimir operator for soft induced $g \rightarrow gg$ splitting with $x = 0.03$ at $E = 100$ GeV versus the jet path length obtained for the splitting point (from left to right) $z_s = 0.5, 2, 3.5$ and 5 fm (see main text for details).

direct $N = 1$ rescattering transition of the 8_A state to the decuplet states is forbidden. And the leading order in the QGP density $N = 2$ rescattering contribution comes from the sequential transitions: $8_A \rightarrow 8_S, 27 \rightarrow 10(\overline{10})$.

Besides the probabilities for distinct multiplets it is instructive to examine the z -dependence of the $SU(3)$ -multiplet averaged color Casimir of the gg pair

$$\langle C_2 \rangle = \sum_R P_R C_2[R], \quad (39)$$

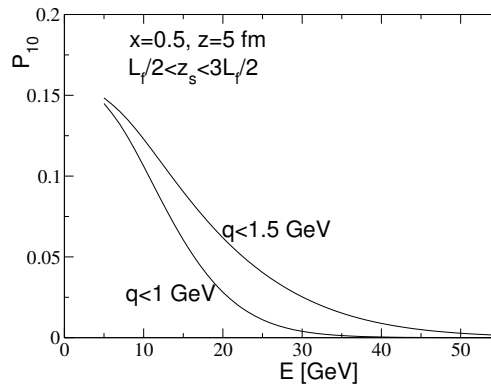


FIG. 13: Energy dependence of the probability of the decuplet state for $q < 1$ and $q < 1.5$ GeV for the typical jet path length in the QGP $z = 5$ fm. The splitting $g \rightarrow gg$ occurs in the region $L_f/2 < z_s < 3L_f/2$.

that may be viewed as a reasonable integral characteristic of the color randomization. Instantly after $g \rightarrow gg$ splitting $\langle C_2 \rangle = C_2[8] = N_c$, and for fully randomized regime $\langle C_2 \rangle = 2C_2[8] = 2N_c$. As was mentioned above, the total Casimir of the gg pair controls the emissions of gluons with the inverse transverse momentum smaller than the transverse size of the gg pair, when it acts as a single radiator. In Fig. 11 we plot the z -dependence of $\langle C_2 \rangle$. As in the figures for P_R , we show the results for the versions with the instant and delayed splitting. From Fig. 11 one sees that $\langle C_2 \rangle$ for the typical jet path length $L \sim 5$ fm for central Pb+Pb collisions differs considerably from its value $2N_c$ for the fully color randomized gg state. At $E = 500$ GeV even at $L = 10$ fm the color randomization is not reached. In this case $\langle C_2 \rangle$ lies in the middle between the values for the pure octet state and for the fully randomized two-gluon state (both for the asymmetric ($x = 0.1$) and symmetric ($x = 0.5$) gluon pairs).

As we said, the approximation of rigid geometry with the straight-line gluon trajectories (the same for amplitude and for the complex conjugate one) seems to be reasonable for a hard $g \rightarrow gg$ splitting. For the soft induced gluon emission the quantum fluctuations of the parton trajectories are important, and the full path integral machinery should be used. In this case the color algebra part of the calculations should be performed before the integrations over the parton trajectories. And the effect of the randomization in the color space and the effect of the fluctuations of the trajectories cannot be separated. Nevertheless, the approximation of rigid geometry seems to be a reasonable method for a qualitative analysis of the color randomization for the induced $g \rightarrow gg$ splitting. To perform such an analysis we use estimates of the local formation length and the transverse momentum squared for induced gluon emission inside the QGP in terms of the transport coefficient \hat{q} (see, e.g. [2, 40]): $k_T^2 \sim \sqrt{2\omega\hat{q}}$, and $L_f^{in} \sim \sqrt{2\omega/\hat{q}}$. We take the local transport coefficient in the form $\hat{q} \approx 2\varepsilon^{3/4} \approx 15T^3$ obtained in [55], which, as we said above, is in a reasonable agreement with our dipole cross section $\sigma_8(\rho)$ at small ρ . For the induced $g \rightarrow gg$ splitting we use the Gaussian transverse momentum distribution $dN/dk^2 \propto \exp(-k_T^2/\langle k_T^2 \rangle)$ with $\langle k_T^2 \rangle = \sqrt{2\omega\hat{q}}$, and the local \hat{q} calculated at $L = z_s + L_f^{in}/2$. In Fig. 12 we present the average Casimir operator for the soft $g \rightarrow gg$ splitting at $E = 100$ GeV for $x = 0.03$ (i.e. at $\omega = 3$ GeV) obtained in this model for the splitting positions in the QGP $z_s = 0.5, 2, 3.5$ and 5 fm. Note that at $x \ll 1$ the results are insensitive to the value of E . From Fig. 12 one can see that even for the induced gluon emission in the initial hottest stage of the QGP the color randomization requires ~ 5 fm. This plot clearly shows that for gluons emitted at later stages ($L \sim 3 - 5$ fm) the color randomization is incomplete even at $L \sim 10$ fm. Thus, our results show that a considerable part of the gluon pairs created in the induced $g \rightarrow gg$ processes may leave the QGP without complete color decoherence.

The formalism of the present paper allows to study quantitatively the energy dependence of the decuplet gg pair production. As we said in introduction, it is important for better understanding of the role of the collinear decuplet two-gluon states in the baryon jet fragmentation due to the mechanism shown in Fig. 2. In Ref. [24] the contribution of this mechanism has been estimated in the approximation of complete color randomization. The analysis of Ref. [24] is based on the calculation of the phase space for formation of the diquark (that is formed from two quarks created after the conversion of both gluons to $q\bar{q}$ pairs, as shown in Fig. 2) with mass $M_D \lesssim 1 - 1.5$ GeV. The diquark configurations with higher values of M_D should have a smaller probability for fragmentation into a leading baryon. The dominating contribution to such diquark states comes from the gluon splitting to symmetric gluon pairs with $x \sim 0.5$ and $q \lesssim 1$ GeV. The qualitative estimates of Ref. [24] show that the approximation of the complete color randomization of the gg pairs should stay reasonable for jets with $E \lesssim 20 - 30$ GeV. The corresponding limit for the baryon momenta is smaller by a factor of $\sim 2 - 3$ (because the diquark momentum is smaller than the jet energy by a factor of ~ 2 , and some part of the longitudinal momentum is lost in the diquark fragmentation to the observed baryon). This means that the contribution of the anomalous color decuplet gg pairs may be potentially important for baryon production at $p_T \lesssim 7 - 10$ GeV. Beyond this p_T region it should decrease steeply due to the fall of the probability to find the gg pair in the decuplet color state. Because for a given q the angle between gluons $\propto 1/E$ and the transverse size of the gg pair also decreases $\propto 1/E$. As a result, the probability of excitation of the decuplets states should fall steeply with E , as was already said in Sec. 3. However, of course, the estimates of Ref. [24] are very crude. We use our formalism to perform a quantitative analysis. In Fig. 13 we plot the energy dependence of the probability of the decuplet state for $q < 1$ and $q < 1.5$ GeV for $L = 5$ fm, which is the typical jet path length in the QGP for central Pb+Pb collisions. The curves are obtained for the splitting $g \rightarrow gg$ in the region $L_f/2 < z_s < 3L_f/2$. From Fig. 13 one sees that for jets with $E \sim 5 - 7$ GeV P_{10} is close to that for full color randomization, i.e. $P_{10} = 10/64$, and from $E \sim 10$ GeV to $E \sim 30$ GeV P_{10} falls steeply. In terms of the baryon transverse momentum it means the anomalous contribution of the baryon production becomes small at $p_T \gtrsim 10 - 15$ GeV. This is in agreement with the recent data from ALICE [32] on the high- p_T spectra in Pb+Pb collisions at $\sqrt{s} = 2.76$ TeV that show that the ratio $(p+\bar{p})/(\pi^++\pi^-)$ becomes close to that for pp collisions at $p_T \gtrsim 10 - 15$ GeV. The steep decrease of the probability for production of the decuplet gg states is a consequence of the fact that the excitation of the decuplet state requires, as was said before, at least two rescatterings and growth of the formation length (that leads to reduction of the effective path length of the gg pair in the QGP).

V. CONCLUSIONS

In this paper we have studied the dynamics of the color randomization of two-gluon states produced after splitting of a primary fast gluon in the QGP formed in heavy ion collisions. Numerical calculations have been performed for central Pb+Pb collisions at the LHC energy $\sqrt{s} = 2.76$ TeV. The analysis is based on the evolution equation for the color density matrix for gg system obtained in the dipole approach. In our framework the density matrix of the two-gluon pair may be viewed as wave function of a color singlet four-gluon system. The L -dependence of this wave function is controlled by the diffraction operator for scattering of the four-gluon system on the QGP constituents. We have found that the color randomization of the gg pairs turns out to be rather slow. Our calculations show that for jet energies $E = 100$ and 500 GeV the $SU(3)$ -multiplet averaged color Casimir C_2 of the gg state for the typical jet path length $L \sim 5$ fm for central Pb+Pb collisions differs considerably from its value $2N_c$ for the fully color randomized gg state. For jets with $E = 500$ GeV even at $L = 10$ fm the color randomization is not reached. In this case the averaged color Casimir lies in the middle between the values for the pure octet state (as for the parent gluon) and for the fully randomized two-gluon state (both for the asymmetric ($x = 0.1$) and symmetric ($x = 0.5$) gluon pairs).

We have found that the rate of the color randomization is slowest for the decuplet color multiplets: 10 and $\overline{10}$. This occurs because, contrary to other states in the Clebsch-Gordan decomposition of the direct product of two octets, the direct transition $8_A \rightarrow 10(\overline{10})$ for $N = 1$ rescattering is forbidden, and the excitation of the decuplet states goes through excitation of the intermediate 8_S and 27 multiplets.

We have studied the energy dependence of the generation of the nearly collinear decuplet gg states, that can lead to production of leading baryons in jet fragmentation [24, 27]. We find that the probability to observe such pairs decreases steeply with jet energy, and becomes very small for $E \gtrsim 30$ GeV. It allows one to conclude that the contribution of this mechanism to the baryon production should become very small at $p_T \sim 10$ GeV. This agrees reasonably with the data from ALICE [32] on the ratio $(p + \bar{p})/(\pi^+ + \pi^-)$ in Pb+Pb collisions at $\sqrt{s} = 2.76$ TeV.

Acknowledgments

This work has been supported by the RScF grant 16-12-10151.

Appendix

The contribution to the two-gluon color wave function $\langle ab|\Psi\rangle$ of a given irreducible $SU(3)$ multiplet R in the Clebsch-Gordan decomposition (4) can be written as $P[R]_{cd}^{ab}\langle cd|\Psi\rangle$, where $P[R]$ is the projector operator for the multiplet R given by the general quantum mechanical formula (14). The projectors onto the multiplets 1 , 8_A , 8_S , 27 , 10 and $\overline{10}$ can be written in terms of the Kronecker deltas, antisymmetric tensor f_{abc} and symmetric tensor d_{abc} as

$$P[1]_{cd}^{ab} = \frac{1}{8}\delta_{ab}\delta_{cd}, \quad (40)$$

$$P[8_A]_{cd}^{ab} = \frac{1}{3}f_{abk}f_{kcd}, \quad (41)$$

$$P[8_S]_{cd}^{ab} = \frac{3}{5}d_{abk}d_{kcd}, \quad (42)$$

$$P[27]_{cd}^{ab} = \frac{1}{2}(\delta_{ac}\delta_{bd} + \delta_{ad}\delta_{bc}) - \frac{1}{8}\delta_{ab}\delta_{cd} - \frac{3}{5}d_{abk}d_{kcd}, \quad (43)$$

$$P[10]_{cd}^{ab} = \frac{1}{4}(\delta_{ac}\delta_{bd} - \delta_{ad}\delta_{bc}) - \frac{1}{6}f_{abk}f_{kcd} + \frac{i}{2}Y_{cd}^{ab}, \quad (44)$$

$$P[\overline{10}]_{cd}^{ab} = \frac{1}{4}(\delta_{ac}\delta_{bd} - \delta_{ad}\delta_{bc}) - \frac{1}{6}f_{abk}f_{kcd} - \frac{i}{2}Y_{cd}^{ab}, \quad (45)$$

where

$$Y_{cd}^{ab} = -\frac{1}{2}(d_{ack}f_{kbd} + f_{ack}d_{kbd}). \quad (46)$$

The two-gluon color wave function for the states 1 , 8_S , 27 are symmetric in permutations of gluon color indexes $a \leftrightarrow b$ and $c \leftrightarrow d$, and the states 8_A , 10 , $\bar{10}$ are antisymmetric. The contribution of the first three terms in the formulas for the decuplet projectors is clearly antisymmetric, the fact that the term Y_{cd}^{bc} is also antisymmetric for $a \leftrightarrow b$ and $c \leftrightarrow d$ is evident from the identity

$$d_{ack}f_{kdb} + f_{ack}d_{kdb} = d_{cbk}f_{kda} + f_{cbk}d_{kda}. \quad (47)$$

Calculations of the projectors for 1 , 8_S , 27 and 8_A multiplets are trivial, but for 10 and $\bar{10}$ multiplets they are more complicated. The projectors $P[10]$ and $P[\bar{10}]$ can be obtained after straightforward (somewhat tedious) calculations with the help of the standard formula (14) using for the decuplet (antidecuplet) states the symmetric spinor tensors Ψ^{ijk} (Ψ_{ijk}). For the two-gluon state these tensors can be built using the spinor form of the gluon wave function $(g_a)_k^i = \frac{1}{\sqrt{2}}(\lambda_a)_k^i$.

An important fact for our calculations is that the projectors are proportional to the four-gluon color wave functions of the color singlets $|R\bar{R}\rangle$ built from R and \bar{R} multiplets (16). The fact that the wave function given by (16) describes a color singlet can be checked by calculating the expectation value

$$\langle R\bar{R}|T^\alpha|R\bar{R}\rangle \quad (48)$$

of the total color generator $T^\alpha = \sum_{i=1}^4 T_i^\alpha$ for four gluons, which should vanish for color singlet states. One can easily show that this is true. Indeed, say, for the contribution from $i = 1$ we have

$$\langle R\bar{R}|T_1^\alpha|R\bar{R}\rangle \propto (P[R]_{cd}^{a'b})^* f_{\alpha a'a} P[R]_{cd}^{ab}. \quad (49)$$

Since $(P[R]_{cd}^{a'b})^* = P[R]_{a'b}^{cd}$ and $P[R]_{cd}^{ab} P[R]_{a'b}^{cd} = P[R]_{a'b}^{ab} \propto \delta_{aa'}$ one can see that the left-hand side of (49) $\propto f_{\alpha aa} = 0$. The fact that the projector operator (14) is proportional to the color singlet wave function $|R\bar{R}\rangle$ is not surprising, because the last factor on the right-hand side of (14) is proportional to the wave function of the complex conjugate state $\langle cd|\bar{R}\bar{\nu}\rangle$ (where the component $\bar{\nu}$ has the “magnetic” quantum numbers opposite to that for ν) with the phase factor similar to that in the Clebsch-Gordan sum over the internal quantum number ν for the color singlet state $R\bar{R}$ [57, 58] built from the states $|R\nu\rangle$ and $|\bar{R}\bar{\nu}\rangle$.

The crossing operator U_{ts} from the s -channel basis to the t -channel one can be calculated with the help of the above formulas for the s -channel projectors and similar formulas for the t -channel basis (that can be obtained by permuting $b \leftrightarrow c$). However, the crossing operation involves also the mixed states $|8_A 8_S\rangle$ and $|8_S 8_A\rangle$. It is convenient to use the linear combinations (26), and take the wave functions for the components $|8_A 8_S\rangle$ and $|8_S 8_A\rangle$ in the s -channel basis in the form

$$\langle abcd|8_A 8_S\rangle = \frac{1}{\sqrt{40}} f_{abk} d_{kcd}, \quad \langle abcd|8_S 8_A\rangle = \frac{1}{\sqrt{40}} d_{abk} f_{kcd}. \quad (50)$$

Similar formulas for the t -channel basis are obtained by interchanging $b \leftrightarrow c$. A straightforward calculation gives

$$\begin{pmatrix} |11\rangle \\ |8_A 8_A\rangle \\ |8_S 8_S\rangle \\ |2727\rangle \\ |10\bar{10}\rangle \\ |\bar{10}10\rangle \\ |(8_A 8_S)_+\rangle \\ |(8_A 8_S)_-\rangle \end{pmatrix}_t = \begin{pmatrix} \frac{1}{8} & \frac{1}{\sqrt{8}} & \frac{1}{\sqrt{8}} & \frac{3\sqrt{3}}{8} & \frac{\sqrt{5}}{4\sqrt{2}} & \frac{\sqrt{5}}{4\sqrt{2}} & 0 & 0 \\ \frac{1}{\sqrt{8}} & \frac{1}{2} & \frac{1}{2} & -\frac{\sqrt{3}}{2\sqrt{2}} & 0 & 0 & 0 & 0 \\ \frac{1}{\sqrt{8}} & \frac{1}{2} & -\frac{3}{10} & \frac{3\sqrt{3}}{10\sqrt{2}} & -\frac{1}{\sqrt{5}} & -\frac{1}{\sqrt{5}} & 0 & 0 \\ \frac{3\sqrt{3}}{8} & -\frac{\sqrt{3}}{2\sqrt{2}} & \frac{3\sqrt{3}}{10\sqrt{2}} & \frac{7}{40} & -\frac{\sqrt{3}}{4\sqrt{10}} & -\frac{\sqrt{3}}{4\sqrt{10}} & 0 & 0 \\ \frac{\sqrt{5}}{4\sqrt{2}} & 0 & -\frac{1}{\sqrt{5}} & -\frac{\sqrt{3}}{4\sqrt{10}} & \frac{1}{4} & \frac{1}{4} & -\frac{1}{\sqrt{2}} & 0 \\ \frac{\sqrt{5}}{4\sqrt{2}} & 0 & -\frac{1}{\sqrt{5}} & -\frac{\sqrt{3}}{4\sqrt{10}} & \frac{1}{4} & \frac{1}{4} & \frac{1}{\sqrt{2}} & 0 \\ 0 & 0 & 0 & 0 & -\frac{1}{\sqrt{2}} & \frac{1}{\sqrt{2}} & 0 & 0 \\ 0 & 0 & 0 & 0 & 0 & 0 & 0 & -1 \end{pmatrix} \times \begin{pmatrix} |11\rangle \\ |8_A 8_A\rangle \\ |8_S 8_S\rangle \\ |2727\rangle \\ |10\bar{10}\rangle \\ |\bar{10}10\rangle \\ |(8_A 8_S)_+\rangle \\ |(8_A 8_S)_-\rangle \end{pmatrix}_s \quad (51)$$

As one can see the crossing matrix is real and symmetrical.

A straightforward calculation of the 6×6 diffraction matrix in the s -channel basis with the help of the above formulas for the projectors gives (the order of states is the same as in (10))

$$\hat{\sigma}(\rho) = \sigma_8(\rho) \times \begin{pmatrix} 2 & -\frac{1}{\sqrt{2}} & 0 & 0 & 0 & 0 \\ -\frac{1}{\sqrt{2}} & \frac{3}{2} & -\frac{1}{2} & -\frac{1}{\sqrt{6}} & 0 & 0 \\ 0 & -\frac{1}{2} & \frac{3}{2} & 0 & -\frac{1}{\sqrt{5}} & -\frac{1}{\sqrt{5}} \\ 0 & -\frac{1}{\sqrt{6}} & 0 & \frac{2}{3} & -\frac{2}{\sqrt{30}} & -\frac{2}{\sqrt{30}} \\ 0 & 0 & -\frac{1}{\sqrt{5}} & -\frac{2}{\sqrt{30}} & 1 & 0 \\ 0 & 0 & -\frac{1}{\sqrt{5}} & -\frac{2}{\sqrt{30}} & 0 & 1 \end{pmatrix}, \quad (52)$$

where $\sigma_8(\rho)$ is the dipole cross section for a color singlet two-gluon system of the size ρ .

-
- [1] M. Gyulassy and X.N. Wang, Nucl. Phys. B**420**, 583 (1994) [nucl-th/9306003].
 - [2] R. Baier, Y.L. Dokshitzer, A.H. Mueller, S. Peigné and D. Schiff, Nucl. Phys. B**483**, 291 (1997) [hep-ph/9607355]; *ibid.* B**484**, 265 (1997) [hep-ph/9608322].
 - [3] B.G. Zakharov, JETP Lett. **63**, 952 (1996) [hep-ph/9607440]; Phys. Atom. Nucl. **61**, 838 (1998) [hep-ph/9807540].
 - [4] M. Gyulassy, P. Lévai and I. Vitev, Nucl. Phys. B**594**, 371 (2001) [hep-ph/0006010].
 - [5] P. Arnold, G.D. Moore and L.G. Yaffe, JHEP **0206**, 030 (2002) [hep-ph/0204343].
 - [6] U.A. Wiedemann, Nucl. Phys. A**690**, 731 (2001) [hep-ph/0008241].
 - [7] J.D. Bjorken, Fermilab preprint 82/59-THY (1982, unpublished).
 - [8] B.G. Zakharov, JETP Lett. **86**, 444 (2007) [arXiv:0708.0816].
 - [9] G.-Y. Qin, J. Ruppert, C. Gale, S. Jeon, G.D. Moore and M.G. Mustafa, Phys. Rev. Lett. **100**, 072301 (2008) [arXiv:0710.0605].
 - [10] R. Baier, Yu.L. Dokshitzer, A.H. Mueller and D. Schiff, JHEP **0109**, 033 (2001).
 - [11] B.G. Zakharov, JETP Lett. **70**, 176 (1999) [hep-ph/9906536].
 - [12] B.G. Zakharov, JETP Lett. **73**, 49 (2001) [hep-ph/0012360].
 - [13] P. Arnold and S. Iqbal, JHEP **1504**, 070 (2015), Erratum: JHEP **1609**, 072 (2016) [arXiv:1501.04964].
 - [14] P. Arnold, H.-C. Chang and S. Iqbal, JHEP **1610**, 100 (2016) [arXiv:1606.08853].
 - [15] P. Arnold, H.-C. Chang and S. Iqbal, JHEP **1610**, 124 (2016) [arXiv:1608.05718].
 - [16] K. Zapp, G. Ingelman, J. Rathsman, J. Stachel and U.A. Wiedemann, Eur. Phys. J. C**60**, 617 (2009) [arXiv:0804.3568].
 - [17] K.C. Zapp, F. Krauss and U.A. Wiedemann, JHEP **1303**, 080 (2013) [arXiv:1212.1599].
 - [18] I.P. Lokhtin, A.V. Belyaev and A.M. Snigirev, Eur. Phys. J. C**71**, 1650 (2011) [arXiv:1103.1853].
 - [19] S. Cao *et al.* [JETSCAPE Collaboration] Phys. Rev. C**96**, 024909 (2017) [arXiv:1705.00050].
 - [20] P. Lévai and U. Heinz, Phys. Rev. C**57**, 1879 (1998).
 - [21] H. Song, S.A. Bass, U. Heinz, and T. Hirano, Phys. Rev. C**83**, 054910 (2011), Erratum: Phys. Rev. C**86**, 059903 (2012) [arXiv:1101.4638].
 - [22] B.G. Zakharov, JETP Lett. **88**, 781 (2008) [arXiv:0811.0445].
 - [23] A. Leonidov and V. Nechitailo, Eur. Phys. J. C**71**, 1537 (2011) [arXiv:1006.0366].
 - [24] P. Aurenche and B.G. Zakharov, Eur. Phys. J. C**71**, 1829 (2011) [arXiv:1109.6819].
 - [25] A. Beraudo, J.G. Milhano and U.A. Wiedemann, JHEP **1207**, 144 (2012) [arXiv:1204.4342].
 - [26] A. Beraudo, J.G. Milhano and U.A. Wiedemann, Phys. Rev. C**85**, 031901 (2012) [arXiv:1109.5025].
 - [27] B.G. Zakharov, Proceedings of the 33rd Rencontres de Moriond: QCD and High Energy Hadronic Interactions, Les Arcs, France, March 21-28, 1998, pp. 465-469 [arXiv:hep-ph/9807396].
 - [28] G.C. Rossi and G. Veneziano, Nucl. Phys. B**123**, 507 (1977).
 - [29] G.C. Rossi and G. Veneziano, Phys. Rep. **63**, 149 (1980).
 - [30] B.I. Abelev *et al.* [STAR Collaboration], Phys. Rev. Lett. **97**, 152301 (2006) [nucl-ex/0606003].
 - [31] S.S. Adler *et al.* [PHENIX Collaboration], Phys. Rev. Lett. **91**, 172301 (2003) [nucl-ex/0305036].
 - [32] J. Adam *et al.* [ALICE Collaboration], Phys. Rev. C**93**, 034913 (2016) [arXiv:1506.07287].
 - [33] Y. Mehtar-Tani, C.A. Salgado and K. Tywoniuk, Phys. Lett. B**707**, 156 (2012) [arXiv:1102.4317].
 - [34] J. Casalderrey-Solana and E. Iancu, J. Phys. G**38**, 124062 (2011) [arXiv:1106.3864].
 - [35] J. Casalderrey-Solana and E. Iancu, JHEP **1108**, 015 (2011) [arXiv:1105.1760].
 - [36] M.R. Calvo, M.R. Moldes and C.A. Salgado, Phys. Lett. B**738**, 448 (2014) [arXiv:1403.4892].
 - [37] Basics of perturbative QCD Y.L. Dokshitzer, V.A. Khoze, A.H. Mueller and S.I. Troian. 1991. Published in Gif-sur-Yvette, France: Ed. Frontieres (1991) 274 p. (Basics of)
 - [38] J. Casalderrey-Solana, Y. Mehtar-Tani, C.A. Salgado and K. Tywoniuk, Phys. Lett. B**725**, 357 (2013) [arXiv:1210.7765].
 - [39] A. Kurkela and U.A. Wiedemann, Phys. Lett. B**740**, 172 (2015) [arXiv:1407.0293].
 - [40] P. Caucal, E. Iancu, A.H. Mueller and G. Soyez, arXiv:1801.09703.
 - [41] N.N. Nikolaev, W. Schafer and B.G. Zakharov, Phys. Rev. D**72**, 114018 (2005) [arXiv:hep-ph/0508310].
 - [42] N. Kidonakis, G. Oderda and G.F. Sterman, Nucl. Phys. B**531**, 365 (1998) [hep-ph/9803241].
 - [43] Yu.L. Dokshitzer and G. Marchesini, Phys. Lett. B**631**, 118 (2005) [hep-ph/0508130].
 - [44] Yu.L. Dokshitzer and G. Marchesini, JHEP **0601**, 007 (2006) [hep-ph/0509078].
 - [45] M.H. Seymour, JHEP **0510**, 029 (2005) [hep-ph/0508305].
 - [46] J.-P. Blaizot, F. Dominguez, E. Iancu and Y. Mehtar-Tani, JHEP **1301**, 143 (2013) [arXiv:1209.4585].
 - [47] L. Apolinario, N. Armesto, J.G. Milhano and C.A. Salgado, JHEP **1502**, 119 (2015) [arXiv:1407.0599].
 - [48] J.D. Bjorken, Phys. Rev. D**27**, 140 (1983).
 - [49] B.G. Zakharov, J. Phys. G**40**, 085003 (2013) [arXiv:1304.5742].
 - [50] B.G. Zakharov, J. Phys. G**41**, 075008 (2014) [arXiv:1311.1159].
 - [51] B. Müller and K. Rajagopal, Eur. Phys. J. C**43**, 15 (2005).
 - [52] O. Kaczmarek and F. Zantow, Phys. Rev. D**71**, 114510 (2005) [hep-lat/0503017].
 - [53] N.N. Nikolaev and B.G. Zakharov, Phys. Lett. B**327**, 149 (1994).

- [54] Yu.L. Dokshitzer, V.A. Khoze and S.I. Troyan, Phys. Rev. D **53**, 89 (1996).
- [55] R. Baier, Nucl. Phys. A **715**, 209 (2003) [hep-ph/0209038].
- [56] E.V. Shuryak, Rev. Mod. Phys. **65**, 1 (1993).
- [57] J.J. deSwart, Rev. Mod. Phys. **35**, 916 (1963).
- [58] C. Rebbi and R. Slansky, Rev. Mod. Phys. **42**, 68 (1970).